TRANSVERSE NUCLEON STRUCTURE AND MULTIPARTON INTERACTIONS*

Mark Strikman

Penn State University, University Park, PA 16802, USA

(Received November 7, 2011)

The transverse structure of the nucleon as probed in hard exclusive processes plays critical role in the understanding of the structure of the underlying event in hard collisions at the LHC, and multiparton interactions. We summarize results of our recent studies of manifestation of transverse nucleon structure in the hard collisions at the LHC, new generalized parton distributions involved in multiparton interactions, presence of parton fluctuations. The kinematic range where interaction of fast partons of the projectile with the target reach black disk regime (BDR) strength is estimated. We demonstrate that in the BDR postselection effect leads to effective fractional energy losses. This effect explains regularities of the single and double forward pion production in dAu collisions at RHIC and impacts on the forward physics in pp collisions at the LHC.

DOI:10.5506/APhysPolB.42.2607
PACS numbers: 12.38.–k, 12.38.Qk

1. Introduction

The start of the LHC puts at a forefront the task of the describing the high energy proton–proton collision events in the whole their complexity. In particular, to search for new particles it is necessary to understand the structure of the underlying structure of events with dijets. The knowledge of the inclusive cross-sections of hard binary collisions, which are expressed through the convolution of the hadron parton distribution functions (PDFs) and the hard parton–parton interaction cross-section, is not sufficient for these purposes.

A natural framework for description of the complete picture of the high energy interaction is the impact parameter representation of the collision. Indeed, in high energy pp scattering angular momentum conservation implies that the impact parameter b becomes a good quantum number, and it

* Presented at the LI Cracow School of Theoretical Physics "Soft Side of the LHC", Zakopane, Poland, June 11–19, 2011.

is natural to consider amplitudes and cross-sections in the impact parameter representation. The nucleon's light-cone wave functions, describing the partonic structure at a low resolution scale, can be expressed in terms of the longitudinal momentum fractions of the partons and their transverse positions relative to the center-of-momentum: $\psi_p(x_i, \rho_i)$.

The studies of exclusive hard processes lead to the conclusion that the transverse distribution of gluons with $x \geq 10^{-3}$ than the distribution of soft partons involved in generic inelastic pp collisions (Secs. 2 and 3). As a result, the events with a dijet trigger should occur, in average, at much smaller impact parameters than the minimum-bias inelastic events — see Fig. 1. Probability of multiple soft and hard interactions is much higher for head-on collisions than for peripheral collisions. Hence one expects a much more active final states for the dijet triggered events than for the minimum-bias events.

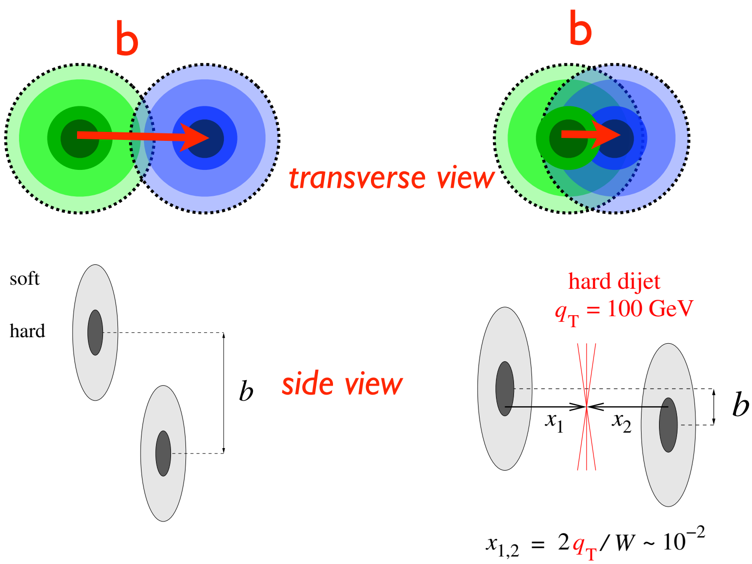

Fig. 1. pp collisions at small and large impact parameters. Transverse and side views. Dark (gray) disks correspond to the areas occupied by hard (soft) partons.

To describe the transverse geometry of the pp collisions with production of a dijet it is convenient to consider probability to find a parton with given x and transverse distance $\vec{\rho}$ from the nucleon center of mass, $f_i(x_i, \vec{\rho}_i)$. This quantity allows a formal operator definition, and it is referred to as the diagonal generalized parton distribution (GPD). It is related to non-diagonal GPDs which enter in the description of the exclusive meson production (Sec. 2). The transverse geometry of the pp collision with production of a dijet is represented in Fig. 2.

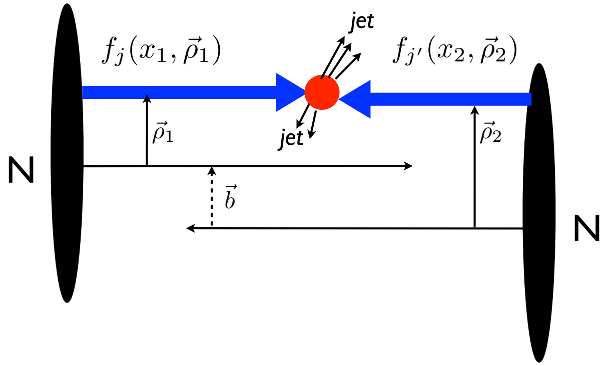

Fig. 2. Transverse geometry of hard collisions.

For inclusive cross-section in the pQCD regime the transverse structure does not matter — the cross-section is expressed through the convolution of parton densities. Indeed, we can write

$$\begin{aligned}\sigma_h &\propto \int d^2bd^2\rho_1 d^2\rho_2 \delta(\rho_1 + b - \rho_2) f_1(x_1, \rho_1) f_2(x_2, \rho_2)\sigma_{2\to 2}\\ &= \int d^2bd^2\rho_1 d^2\rho_2 f_1(x_1, \rho_1) f_2(x_2, \rho_2)\sigma_{2\to 2} = f_1(x_1) f_2(x_2)\sigma_{2\to 2}\,. \quad (1)\end{aligned}$$

Here at the last step we used the relation between diagonal GPD and PDF $\int d^2\rho f_j(x, \rho, Q^2) = f_j(x, Q^2)$.

At the same time, as soon as one wants to describe the structure of the final state in production of say heavy particles, it is important to know whether a dijet production occurs at different average impact parameters than the minimum-bias interactions. We will argue below that dijet trigger selects, in average, a factor of two smaller impact parameters. This implies that the multijet activity, energy flow should be much stronger in these events than in the minimum-bias events. Obviously, the magnitude of the enhancement does depend on the transverse distribution of partons and on correlation between the partons in the transverse plane. This information becomes available now.

2. Transverse structure of the nucleon wave function

The basis for the quantitative analysis of the transverse nucleon structure is provided by the QCD factorization theorem for exclusive vector meson (VM) production [1] which states that in the leading twist approximation the differential cross-section of the process $\gamma_L^* + p \to \mathrm{VM} + p$ is given by the convolution of the hard block, meson wave function and generalized gluon parton distribution, $g(x_1, x_2, t \,|\, Q^2)$, where x_1, x_2 are the longitudinal momentum fractions of the emitted and absorbed gluon (we discuss here only the case of small x which is of relevance for the LHC kinematics). Of particular interest is the generalized parton distribution (GPD) in the "diagonal" case, $g(x, t|Q^2)$, where $x_1 = x_2$ and denoted by x, and the momentum transfer to the nucleon is in the transverse direction, with $t = -\boldsymbol{\Delta}_\perp^2$ (we follow the notation of Refs. [2,3]). This function reduces to the usual gluon density in the nucleon in the limit of zero momentum transfer, $g(x, t = 0|Q^2) = g(x|Q^2)$. Its two-dimensional Fourier transform

$$g\left(x, \rho|Q^2\right) \equiv \int \frac{d^2\Delta_\perp}{(2\pi)^2}\, e^{i(\boldsymbol{\Delta}_\perp \boldsymbol{\rho})}\, g\left(x, t = -\boldsymbol{\Delta}_\perp^2|Q^2\right) \tag{2}$$

describes the one-body density of gluons with given x in transverse space, with $\rho \equiv |\boldsymbol{\rho}|$ measuring the distance from the transverse center-of-momentum of the nucleon, and is normalized such that $\int d^2\rho\, g(x, \rho|Q^2) = g(x|Q^2)$. It is convenient to separate the information on the total density of gluons from their spatial distribution and parametrize the GPD in the form

$$g\left(x, t|Q^2\right) = g\left(x|Q^2\right)\; F_g\left(x, t|Q^2\right)\,, \tag{3}$$

where the latter function satisfies $F_g(x, t = 0|Q^2) = 1$ and is known as the two-gluon form factor of the nucleon. Its Fourier transform describes the normalized spatial distribution of gluons with given x,

$$F_g\left(x, \rho|Q^2\right) \equiv \int \frac{d^2\Delta_\perp}{(2\pi)^2}\, e^{i(\boldsymbol{\Delta}_\perp \boldsymbol{\rho})}\, F_g\left(x, t = -\boldsymbol{\Delta}_\perp^2|Q^2\right)\,, \tag{4}$$

with $\int d^2\rho\, F_g(x, \rho|Q^2) = 1$ for any x.

The QCD factorization theorem predicts that the t-dependence of the VM production should be a universal function of t for fixed x (up to small DGLAP evolution effects). Indeed the t-slope of the J/ψ production is practically Q^2 independent, while the t-slope of the production light vector mesons approaches that of J/ψ for large Q^2. The t-dependence of the measured differential cross-sections of exclusive processes at $|t| < 1\,\mathrm{GeV}^2$ is commonly described either by an exponential, or by a dipole form inspired by analogy with the nucleon elastic form factors. Correspondingly, we consider here two parametrizations of the two-gluon form factor

$$F_g\left(x, t|Q^2\right) = \begin{cases} \exp\left(B_g t/2\right)\,, \\ \left(1 - t/m_g^2\right)^{-2}\,, \end{cases} \tag{5}$$

where the parameters B_g and m_g are functions of x and Q^2. The two parametrizations give very similar results if the functions are matched at

$|t| = 0.5\,\text{GeV}^2$, where they are best constrained by present data (see Fig. 3 of Ref. [4]); this corresponds to [3]

$$B_g = 3.24/m_g^2\,. \tag{6}$$

The analysis of the HERA exclusive data leads to

$$B_g(x) = B_{g0} + 2\alpha'_g\,\ln(x_0/x)\,, \tag{7}$$

where $x_0 = 0.0012, B_{g0} = 4.1\ (^{+0.3}_{-0.5})\ \text{GeV}^{-2}, \alpha'_g = 0.140\ (^{+0.08}_{-0.08})\ \text{GeV}^{-2}$ for $Q_0^2 \sim 3\ \text{GeV}^2$. For fixed x, $B(x,Q^2)$ slowly decreases with increase of Q^2 due to the DGLAP evolution [2]. The uncertainties in parentheses represent a rough estimate based on the range of values spanned by the H1 and ZEUS fits, with statistical and systematic uncertainties added linearly. This estimate does not include possible contributions to α'_g due to the contribution of the large size configurations in the vector mesons and changes in the evolution equation at $-t$ comparable to the intrinsic scale. Correcting for these effects may lead to a reduction of α'_g and hence to a slower increase of the area occupied by gluons with decrease of x.

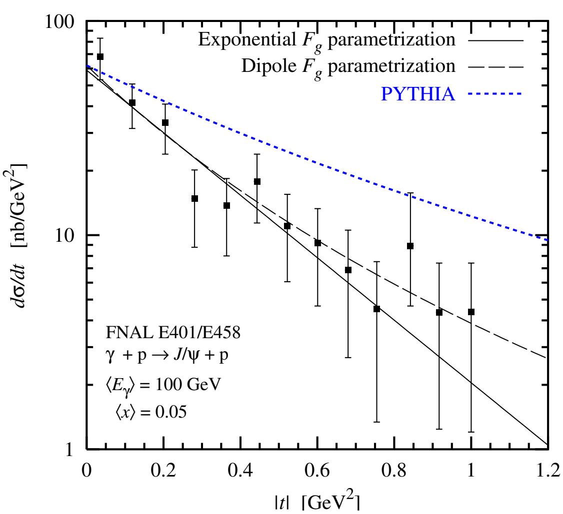

Fig. 3. t-dependence of the exclusive J/ψ photoproduction data from the FNAL E401/458 experiment [5]. Solid line: t-dependence obtained with the exponential parametrization of the two-gluon form factor, Eq. (5) (the slope of the J/ψ cross-section is $B_{J/\psi} = B_g + \Delta B$, where $\Delta B \approx 0.3\ \text{GeV}^{-2}$ accounts for the finite size of the J/ψ; see [3] for details). Dashed line: t-dependence obtained with the dipole parametrization, Eq. (5). Dotted line: t-dependence obtained with PYTHIA, effectively corresponding to a dipole form factor with $m^2 \approx 2\ \text{GeV}^2$.

It is worth noting here that the popular Monte Carlo description of the pp collisions at the collider energies — PYTHIA uses x-independent transverse distribution of partons described by the sum of two exponentials. This distribution roughly equivalent to the dipole parametrization with $m^2 \approx 2\ \text{GeV}^2$ [6] which is hardly consistent with the data on J/ψ photoproduction, see dashed line in Fig. 3. For smaller x the difference is even larger since the transverse size increases with decrease of x — see Eq. (7).

3. Impact parameter distribution of proton–proton collisions with dijet production

Using the information on the transverse spatial distribution of partons in the nucleon, one can infer the distribution of impact parameters in pp collisions with hard parton–parton processes [2]. It is given by the overlap of two parton wave function as depicted in Fig. 4.

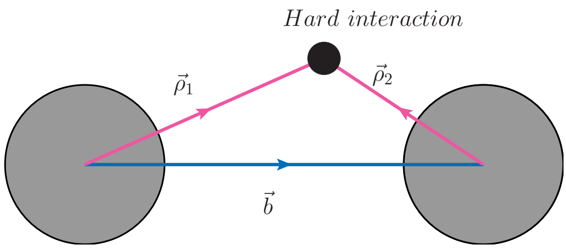

Fig. 4. Overlap integral of the transverse spatial parton distributions, defining the impact parameter distribution of pp collisions with a hard parton–parton process, Eq. (8).

The probability distribution of pp impact parameters in events with a given hard process, $P_2(x_1, x_2, b|Q^2)$, is given by the ratio of the cross-section at given b and the cross-section integrated over b. As a result,

$$P_2\left(x_1, x_2, b|Q^2\right) \equiv \int d^2\rho_1 \int d^2\rho_2\, \delta^{(2)}(\boldsymbol{b} - \boldsymbol{\rho}_1 + \boldsymbol{\rho}_2) \times F_g\left(x_1, \rho_1|Q^2\right)\, F_g\left(x_2, \rho_2|Q^2\right) \tag{8}$$

which, obviously, satisfies the normalization condition

$$\int d^2b\, P_2\left(x_1, x_2, b|Q^2\right) = 1\,. \tag{9}$$

This distribution represents an essential tool for phenomenological studies of the underlying event in pp collisions [2, 3]. We note that the concept of impact parameter distribution is also used in MC generators of pp events with hard processes [7,8], albeit without making the connection with GPDs, which allows one to import information on transverse nucleon structure obtained in the independent measurements.

For the two parametrizations of Eq. (5), Eq. (8) leads to (for $x \equiv x_1 = x_2$)

$$P_2\left(x, b|Q^2\right) = \begin{cases} \left(4\pi B_g\right)^{-1} \exp\left[-b^2/(4B_g)\right] , \\ \left[m_g^2/(12\pi)\right] \left(m_g b/2\right)^3 K_3\left(m_g b\right) , \end{cases} \tag{10}$$

where the parameters B_g and m_g are taken at the appropriate values of x and Q^2.

The derived distribution should be compared to the distribution of the minimum-bias inelastic collisions which could be expressed through $\mathit{\Gamma}(s,b)$ that is the profile function of the pp elastic amplitude ($\mathit{\Gamma}(s,b) = 1$ if the interaction is completely absorptive at given b)

$$P_{\text{in}}(s,b) = \left[1 - |1 - \mathit{\Gamma}(s,b)|^2\right] / \sigma_{\text{in}}(s)\,, \tag{11}$$

where $\int d^2b\, P_{\text{in}}(s,b) = 1$.

Our numerical studies indicate that the impact parameter distributions with the jet trigger (Eq. (10)) are much narrower than that in minimum-bias inelastic events at the same energy (Eq. (11)) and that b-distribution for events with a dijet trigger is a very weak function of the p_{t} of the jets or their rapidities, see Fig. 5. For example, for the case of the pp collisions at $\sqrt{s} = 7$ GeV we find the median value of b, $b_{\text{median}} \approx 1.18$ fm and $b_{\text{median}} \approx 0.65$ fm for minimum-bias and dijet trigger events (Fig. 5 (right)) [3]. Since the large impact parameters give the dominant contribution to σ_{inel} our analysis indicates that there are two pretty distinctive classes of pp collisions — large b collisions which are predominantly soft and central collisions with strongly enhanced rate of hard collisions. We refer to this pattern as the two transverse scale picture of pp collisions at collider energies [2].

A word of caution is necessary here. The transverse distance b for dijet events is defined as the distance between the transverse centers of mass of two nucleons. It may not coincide with b defined for soft interactions where soft partons play an important role. For example, if we consider dijet production due to the interaction of two partons with $x \sim 1$, $\rho_1, \rho_2 \sim 0$ since the transverse center of mass coincides with transverse position of the leading quark in the $x \to 1$ limit. As a result, b for the hard collision will be close to zero. On the other hand, the rest of the partons may interact in this case at different transverse coordinates. As a result, such configurations may contribute to the inelastic pp cross-section at much larger b for the soft interactions. However, for the parton collisions at $x_1, x_2 \ll 1$ the recoil effects are small and so two values of b should be close.

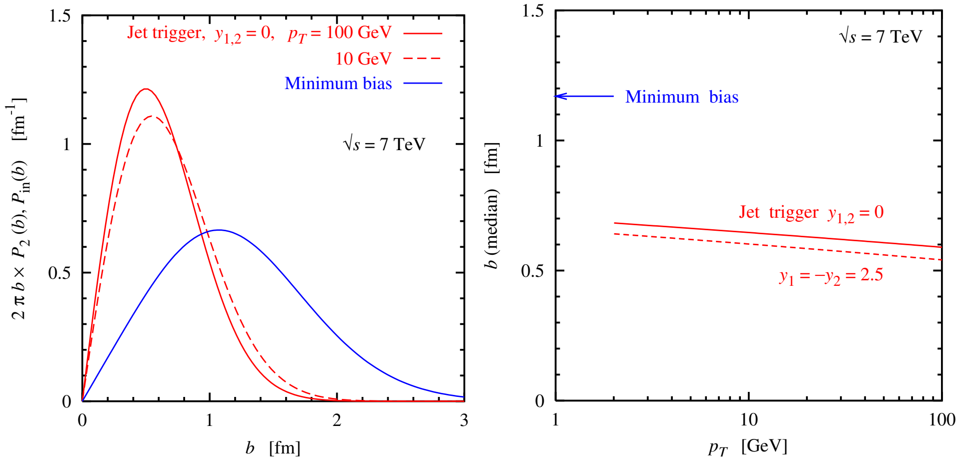

Fig. 5. (Left) Impact parameter distributions of inelastic pp collisions at $\sqrt{s}=7$ TeV. Solid (dashed) line: Distribution of events with a dijet trigger at zero rapidity, $y_{1,2} = 0$, for $p_{\rm t} = 100\,(10)$ GeV *cf.* Eq. (10). Dotted line: Distribution of minimum-bias inelastic events, *cf.* Eq. (11). (Right) Dependence of median b on $p_{\rm t}$ for different rapidities of the dijets.

The present pp LHC data already provide important tests of this picture. Let us consider production of the hadron (minijet) with momentum $p_{\rm t}$. The observable of interest here is the transverse multiplicity, defined as the multiplicity of particles with transverse momenta in a certain angular region perpendicular to the transverse momentum of the trigger particle or jet (the standard choice is the interval $60^\circ < |\Delta\phi| < 120^\circ$ relative to the jet axis; see Ref. [9] for an illustration and discussion of the experimental definition). In the central collisions one expects a much larger transverse multiplicity due to the presence of multiple hard and soft interactions. At the same time, the enhancement should be a weak function of $p_{\rm t}$ in the region, where main contribution is given by the hard mechanism [2, 3]. The predicted increase and eventual flattening of the transverse multiplicity agrees well with the pattern observed in the existing data. At $\sqrt{s} = 0.9$ TeV the transition occurs approximately at $p_{\rm T,\,crit} \approx 4$ GeV, at $\sqrt{s} = 1.8$ TeV at $p_{\rm T,\,crit} \approx 5$ GeV, and at $p_{\rm T,\,crit} = 6$–8 GeV for 7 TeV [10, 11]. We thus conclude that the minimum $p_{\rm t}$ at which particle production, due to hard collisions, starts to dominate significantly increases with the collision energy. This effect is likely to be related to the onset of the high gluon density regime in the central pp interactions, since with an increase of incident energy partons in the central pp, collisions propagate through stronger and stronger gluon fields.

Many further tests of the discussed picture which are suggested in Ref. [3] will be feasible in a near future. They include *(i)* check that the transverse multiplicity does not depend on rapidities of the jets, *(ii)* study of the multiplicity at $y < 0$ for events with jets at $y_1 \sim y_2 \sim 2$. This would allow to check that the transverse multiplicity is universal and that multiplicity in the away and the towards regions is similar to the transverse multiplicity for $y \leq 0$. *(iii)* studying whether transverse multiplicity is the same for quark and gluon induced jets. Since the gluon radiation for production of $W^{\pm}, Z$ is smaller than for the gluon dijets, a subtraction of the radiation effect mentioned below is very important for such a comparisons.

Note that the contribution of the jet fragmentation to the transverse cone, as defined in the experimental analyses, is small but not negligible, especially at smaller energies ($\sqrt{s} = 0.9$ TeV). It would be desirable to use a more narrow transverse cone, or subtract the contribution of the jets fragmentation. Indeed, the color flow contribution [12] leads to a small residual increase of the transverse multiplicity with p_{t}. However, the jet fragmentation effect depends on p_{t} rather than on $\sqrt{s}$. Hence it does not contribute to the growth of the transverse multiplicity, which is a factor of ~ 2 between $\sqrt{s} = 0.9$ TeV and $\sqrt{s} = 7.0$ TeV. In fact, a subtraction of the jet fragmentation contribution would somewhat increase the rate of the increase of the transverse multiplicity in the discussed energy interval. This allows to obtain the lower limit for the rate of the increase of the multiplicity in the central ($\langle b \rangle \sim 0.6$ fm) pp collisions of $s^{0.17}$. It is a bit faster than the s dependence of multiplicity in the central heavy ion collisions.

4. Multiparton interactions

Probability of the multiparton interactions which result in two hard collisions grows rapidly with the increase of the incident energy. Understanding of such processes is important for detailed understanding of the high energy QCD dynamics as well as for practical purposes — estimating backgrounds for the searches for new particles. By exploring the difference in scales between soft and hard QCD processes and space-time structure of Feynman diagrams we derive within pQCD the general formulae for the two dijet production in pp collisions [13, 14] and find that it contains two contributions. The contribution which dominates in a wide range of x_i is the $4 \rightarrow 4$ process which matches the intuitive geometric picture depicted in Fig. 6. However, a consistent pQCD treatment requires that one also takes into account $3 \rightarrow 4$ double hard interaction processes that occur as an interplay between large- and short-distance parton correlations [14]. Such contributions are not taken into consideration by approaches inspired by the parton model picture. This contribution takes into account correlations between the partons induced by the pQCD evolution. Our analysis indicates that this contribution becomes important only for $x \leq 10^{-3}$.

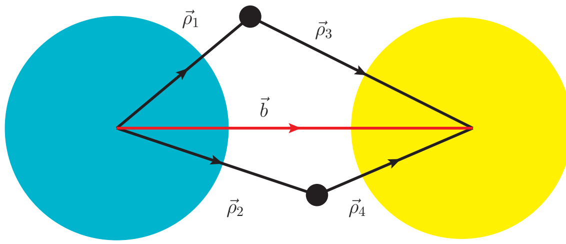

Fig. 6. Geometry of two hard collisions in impact parameter picture.

The $4 \to 4$ cross-section for the collisions of hadrons "a" and "b" has the form [13]

$$d\sigma_4 = \int \frac{d^2\overrightarrow{\Delta}}{(2\pi)^2} \int dx_1 \int dx_2 \int dx_3 \int dx_4$$
$$\times D_a\left(x_1, x_2, p_1^2, p_2^2, \overrightarrow{\Delta}\right) D_b\left(x_3, x_4, p_1^2, p_2^2, -\overrightarrow{\Delta}\right) \frac{d\sigma^{13}}{d\hat{t}_1} \frac{d\sigma^{24}}{d\hat{t}_2} d\hat{t}_1 d\hat{t}_2 \,. \quad (12)$$

Here $D_\alpha(x_1, x_2, p_1^2, p_2^2, \overrightarrow{\Delta})$ are the new "double" GPDs for hadrons "a" and "b"

$$D\left(x_1, x_2, p_1^2, p_2^2, \overrightarrow{\Delta}\right) = \sum_{n=3}^{\infty} \int \frac{d^2k_1}{(2\pi)^2} \frac{d^2k_2}{(2\pi)^2} \theta\left(p_1^2 - k_1^2\right) \theta\left(p_2^2 - k_2^2\right)$$
$$\times \int \prod_{i\neq 1,2} \frac{d^2k_i}{(2\pi)^2} \int_0^1 \prod_{i\neq 1,2} dx_i \, (2\pi)^3 \delta\left(\sum_{i=1}^{i=n} x_i - 1\right) \delta\left(\sum_{i=1}^{i=n} \vec{k}_i\right)$$
$$\times \psi_n\left(x_1, \vec{k}_1, x_2, \vec{k}_2, ., \vec{k}_i, x_i ..\right) \psi_n^+\left(x_1, \overrightarrow{k_1} + \overrightarrow{\Delta}, x_2, \overrightarrow{k_2} - \overrightarrow{\Delta}, x_3, \vec{k}_3, \ldots\right) \,. \quad (13)$$

Note that this distribution is diagonal in the space of all partons except the two partons involved in the collision. Here ψ is the parton wave function normalized to one in the usual way. An appropriate summation over color and Lorentz indices is implied.

Within the parton model approximation the cross-section has the form

$$\sigma_4 = \sigma_1 \sigma_2 / \pi R_{\text{int}}^2 \,, \quad (14)$$

where σ_1 and σ_2 are the cross-sections of two independent hard binary parton interactions. The factor πR_{int}^2 characterizes the transverse area occupied by the partons participating in the two hard collisions. It also includes effect of possible longitudinal correlations between the partons.

Eq. (12) leads to the general model independent expression for

$$\frac{1}{\pi R_{\rm int}^2} = \int \frac{d^2\overrightarrow{\Delta}}{(2\pi)^2} D\left(x_1, x_2, -\overrightarrow{\Delta}\right) D\left(x_1, x_2, \overrightarrow{\Delta}\right) , \tag{15}$$

in terms of two-parton GPDs.

In the independent particle approximation which is used in all Monte Carlo models with multiparton interactions, the two-parton GPD is equal to the product of single particle GPDs discussed in Section 2. Using parametrization of Eq. (10) one finds [2, 13]

$$\frac{1}{\pi R_{\rm int}^2} = \int \frac{d^2\Delta}{(2\pi)^2} F_g^4(\Delta) = \frac{m_g^2}{28\pi} , \tag{16}$$

which leads to approximately a factor of two smaller cross-section than the one observed at the Tevatron: $\pi R_{\rm int}^2 \approx 34$ mb as compared to the experimental value of $\pi R_{\rm int}^2 \approx 15$ mb. The $3 \to 4$ processes play a minor role in the Tevatron kinematics and do not allow to solve this discrepancy.

A fix implemented in the PYTHIA is to assume a much more narrow distribution in ρ-effectively a dipole with $m^2 = 2$ GeV^2. This does decrease $\pi R_{\rm int}^2$ to the value observed at the Tevatron. However, it is a factor of two smaller than the one determined from the analyses of the hard exclusive processes — see discussion in Sec. 2 and, in particular, Fig. 3. Correspondingly, in this model the difference between median ρ^2 for minimum-bias processes and processes with dijet trigger is a factor of 2 larger than what follows from the analysis of the HERA data, *cf.* Fig. 5.

In principle, there is a question of how well the separation of the $2 \to 4$ processes (which is in principle possible [13]) was performed in the experimental studies. However, the most recent D0 analysis [15] seems to indicate that the $2 \to 4$ contribution in the kinematics used to determine $\pi R_{\rm int}^2$ is very small.

This appears to leave us with only one possibility — presence of significant parton–parton correlations at a nonperturbative scale. Currently, we are performing estimates of these correlations. We find that the correlations are indeed large and may explained the enhancement we discussed in this section.

5. Fluctuations of the gluon field and high multiplicity events at LHC

Strength of the gluon field should depend on the size of the quark configurations. For example, the gluon field in the small configurations should be strongly screened — the gluon density much smaller than average. It is possible to extract from the comparison of the diffractive processes:

$\gamma_L^* + p \to V + X$ and $\gamma_L^* + p \to V + p$ the dispersion of the gluon strength at small x [16]

$$\omega_g \equiv \frac{\langle G^2 \rangle - \langle G \rangle^2}{\langle G \rangle^2} = \frac{d\sigma_{\gamma^*+p\to VM+X}}{dt} \Big/ \left.\frac{d\sigma_{\gamma^*+p\to VM+p}}{dt}\right|_{t=0} . \tag{17}$$

The HERA data indicate that for $Q^2 \sim 3$ GeV^2 and $x \sim 10^{-3}$ $\omega_g \sim 0.15 \div 0.2$ which is rather close to the value for the analogous ratio for the soft diffraction which measures fluctuations of overall strength of the *soft* hadronic interactions.

How can one probe the gluon fluctuations in pp collisions? Let us consider multiplicity of an inclusive hard process — dijet, ... as a function of some cuts — for example overall hadron multiplicity: M (trigger) and build the ratio

$$R = \frac{M(\text{trigger})}{M(\text{minimum} - \text{bias})} . \tag{18}$$

If there are no fluctuations of the parton densities, the maximal value of R is reached if the trigger selects collisions at small impact parameters $b \sim 0$. Using Eq. (10) we find [17]

$$R = P_2(0)\sigma_{\text{in}}(pp) = \frac{m_g^2}{12\pi}\sigma_{\text{in}}(pp) \approx 4.5 . \tag{19}$$

Any larger enhancement of R could arise only from the fluctuations of the gluon density per unit area.

The first measurement which may be relevant for addressing the question of fluctuations was reported by ALICE [18]. The multiplicity of J/ψ was studied as a function of the multiplicity in the central detector, namely

$$dN_{\text{ch}}^R/d\eta = \frac{dN_{\text{ch}}/d\eta_{\eta=0}}{\langle dN_{\text{ch}}/d\eta_{\eta=0} \rangle} \tag{20}$$

for $dN_{\text{ch}}^R/d\eta \leq 5$. It was found that R increases with increase of $dN_{\text{ch}}^R/d\eta$ reaching values ≈ 5 for $dN_{\text{ch}}^R/d\eta \sim 4$. This number is close to what we estimated above. Any further increase of R would require presence of the fluctuations in transverse gluon density. An enhancement above the $b = 0$ effect is given by the factor

$$R_{\text{fl}} = \frac{g_N\left(x_1, Q^2|n\right) g_N\left(x_2, Q^2|n\right)}{g_N\left(x_1, Q^2\right) g_N\left(x_2, Q^2\right)} \frac{\langle S \rangle}{S} . \tag{21}$$

Here n labels configurations selected by the trigger, and S is the area of the transverse overlap. In principle, R_{fl} could reach very large values. For example, if we consider a collision of two protons in cigar shape configurations with the same gluon density for different orientations of the protons, the enhancement would be proportional to the ratio of the principal axes of the ellipsoid. Another mechanism for the enhancement of R_{fl} is presence of the dispersion in the gluon density with $\omega_g \sim 0.15 \div 0.2$ (Eq. (17)) which leads to a few percent probability for the gluon field to be a factor 1.5 larger than average.

These observations maybe of relevance for the discussion of the high multiplicity (HM) events studied by the CMS [19]. In the analysis very rare events were selected which have the overall multiplicity for $|\eta| < 2.4$ of at least a factor of ≥ 7 larger than the minimum-bias events. Probability of such events is very small

$$P_{\mathrm{HM}} \approx 10^{-5} \div 10^{-6}\,. \tag{22}$$

The two-particle correlations were measured as a function of the distance in the pseudorapidity — $\Delta\eta$ and the azimuthal angle — $\Delta\phi$. Three types of correlations were observed: (a) very strong local correlation for $\Delta\eta \sim 0$, $\Delta\phi \sim 0$, (b) strong correlation for $\Delta\phi \sim \pi$ for a wide range of $\Delta\eta$, (c) a weak correlation for $2 < |\Delta\eta| < 4.8, \Delta\phi \sim 0$ — so-called ridge.

First question to address is how to get such a large multiplicity. It is pretty obvious that such events should originate from very central collisions. Based on our knowledge of $P_2(b)$ we find that the probability of the collisions at $b < 0.2$ fm is $\sim 2\%$. Using information about dispersion of fluctuations of the gluon fields we estimate the probability of fluctuation, where both nucleons have $g > 1.5 g_N(x)$ is $\geq 10^{-3}$. So a natural guess is that the CMS trigger selected central collisions with enhanced gluon fields in both nucleons. This should lead to a much higher rate of jet production per event.

Indeed our analysis of the HM data indicates presence of a large total excess transverse momentum in the $\Delta\phi \sim \pi$ region: $p_{\mathrm{t}}^{\mathrm{balance}} \geq 15$ GeV$/c$. Presumably, it is due to production of two back-to-back jets with the trigger jet generating the narrow same side correlation. Qualitatively, a large probability of the dijets maybe due to the combination of centrality and the gluon density fluctuation.

Note also that the combination of centrality and jet fragmentation by themselves are not enough to ensure a factor of 7 increase of the multiplicity — without of the gluon density fluctuations these two effects typically lead to $N_{\mathrm{ch}} \sim 70$. The gluon fluctuations would naturally lead to a further increase of N_{ch}.

The same side ridge could originate from the string effect [12]. This could be tested by studying collisions with production of dijets with $p_{\mathrm{t}} \sim 15$ GeV$/c$ without HM trigger. Alternative mechanism would be fluctuations of the transverse shape of the colliding nucleons plus presence of the absorptive effects for $p_{\mathrm{t}} \leq 3$ GeV$/c$. Such a scenario appears quite natural for the high density mechanism we discuss here.

6. Where does the non-linear regime set in?

In the leading log approximation one can derive a relation between the QCD evolution equations and the target rest frame picture of the interaction of small color dipoles with targets expressing it through the gluon density in the target, see [20] and references therein. Matching the behavior of the dipole cross-section in the pQCD regime and of large size dipoles in the regime of soft interaction, it is possible to write interpolation formulae for the dipole–nucleon cross-section for all dipole sizes and describe the total cross-section of DIS at HERA.

To determine how close is the interaction strength to the maximal allowed by the unitarity it is necessary to consider the amplitude of the $q\bar{q}$ dipole–nucleon interaction in the impact parameter space

$$\Gamma_{q\bar{q}}(s,b) = \frac{1}{2is}\frac{1}{(2\pi)^2}\int d^2\vec{q}e^{i\vec{q}\vec{b}}A_{q\bar{q}-N}(s,t)\,, \tag{23}$$

where $A_{q\bar{q}N}(s,t)$ is the elastic amplitude of the $q\bar{q}$ dipole–nucleon scattering normalized to $\mathrm{Im}A_{q\bar{q}N} = is_{q\bar{q}-N}\sigma_{\mathrm{tot}}(q\bar{q}-N)$. The limit $\Gamma_{q\bar{q}}(s,b) = 1$ corresponds to the regime of the complete absorption — black disk regime (BDR) — the maximal strength allowed by the s-channel unitarity.

The t dependence of the $q\bar{q}$ dipole–nucleon elastic scattering amplitude can be obtained from the studies of the exclusive vector meson production in the regime where QCD factorization theorem for the exclusive processes allows to express relate the t dependence of the amplitude to the t-dependence of the gluon GPDs.

Combining this information with the information on the total cross-section of the dipole–nucleon interaction allows us to determine $\Gamma_{q\bar{q}N}(s,b)$ as function of the dipole size. A sample of the results for $q\bar{q}$ dipole–proton interaction which represent an update of the analysis of [21] is presented in Fig. 7. For the case of color octet dipole $\Gamma^{gg}_{\mathrm{inel}} = (9/4)\Gamma^{q\bar{q}}_{\mathrm{inel}}$ leading to Γ^{gg} much closer to one. As a result, the gluon induced interactions are close to the BDR for a much larger range of the dipole sizes (this is consistent with the observation at HERA of a much larger probability of the diffraction in the gluon induce small x DIS processes).

Note also that $\Gamma = 1/2$ already corresponds to a probability of inelastic interaction of $3/4$ which is close to one. One can also show that the inelastic interactions get much larger corrections for the structure of the final states than the total cross-section, see discussion in [22].

In the case of the nuclear target the gain in the value of $\Gamma(b\sim 0)$ is rather small due to the leading twist shadowing. The main gain in the nucleus case is due to a weak dependence of $\Gamma(b)$ on b for a broad range of b.

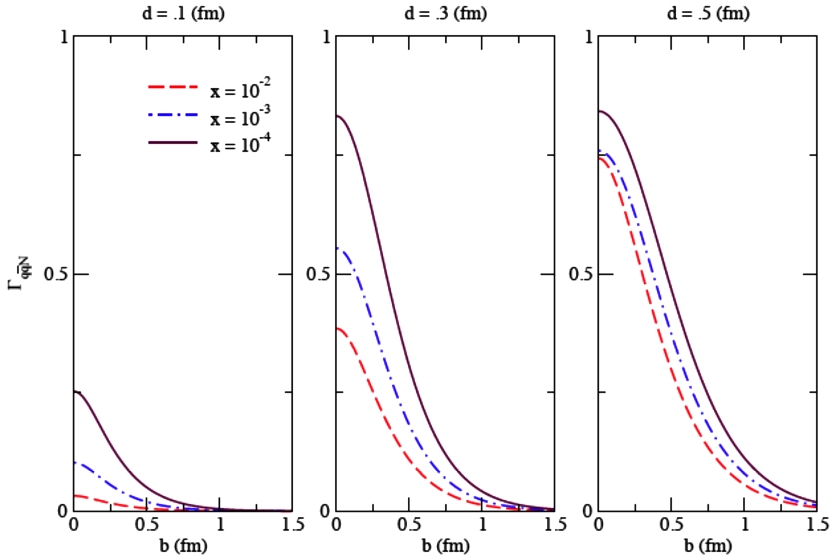

Fig. 7. Impact parameter distribution of $q\bar{q}$ dipole interaction with protons adopted from [21].

Information about $\Gamma_{q\bar{q}-N}(b)$ can be used to estimate the range of the transverse momenta for which probability of the inelastic interaction of parton is close to one [2]. The results of this analysis for $b = 0$ are presented in Fig. 8. One can see from the figure that interaction of gluons is close to the BDR for a wide range of virtualities for the central pp collisions at the LHC.

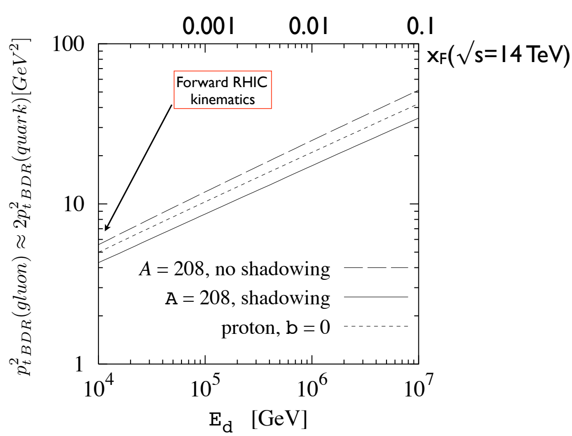

Fig. 8. The $p_{\rm t}$ range where interaction is close to the BDR for the interaction of $q\bar{q}$ and color octet dipoles plotted as a function of the energy of the dipole and of x of the interacting parton for pp interactions at $\sqrt{s} = 14$ TeV.

This is because a parton in the nucleon with a given x_1 resolves the gluons in the second nucleon with x_2 down to $4p_{\rm t}^2/x_1 s$. For example taking $x \sim 10^{-2}$, $\sqrt{s} = 14$ TeV and $\sim p_{\rm t}^2 = 4$ GeV^2 we find $x_2(\min) = 10^{-4}$. Though there are substantial uncertainties in this analysis due to the use of the leading log DGLAP approximation and extrapolation of the gluon densities to very small x, the analysis provides a reasonable estimate of the magnitude of $p_{\rm t}(\mathrm{BDR})$. Note also that the range we find for the RHIC kinematics for the central NA collisions is consistent with the effect of the suppression of the forward pion production due to the onset of the BDR which we discuss in Secs. 8 and 9.

Consequently the LT approximation should be broken for a wide range of x_1, x_2 for gluon–gluon interactions (these are xs for which DGLAP works well for the DIS at HERA). A breakdown of the LT approximation may be of relevance for interpretation of the empirical observation made in a number of the Monte Carlo studies that, to avoid contradictions with the data, one needs to introduce a cutoff for minimal $p_{\rm t}$ of the hard interactions. The cutoff is $p_{\rm t}(\min) \geq 3$ GeV$/c$ for $\sqrt{s} = 7$ TeV and grows with s. In the Monte Carlo models the value of this cutoff is effectively driven by the requirement that the multiplicity of hadrons due to hard interactions remains below the total multiplicity observed experimentally. One can reach similar results (avoiding questions about sensitivity to the hadronization mechanism) based on the calculation of the probability of hard interactions as a function of the impact parameter and requiring that it does not exceed $\varGamma_{\rm inel}(b)$ which is known from the s-channel unitarity [23, 24]. Note, however, that the MC models with $p_{\rm t}(\min)$ cutoff strongly reduce the interactions of the large x partons with the target which contradicts the proximity to the BDR. Hence one may expect that such Monte Carlo models overestimate the cross-section of production of large $x_{\rm F}$ hadrons, especially for the central collisions.

7. Postselection effect in BDR — effective fractional energy losses

It was demonstrated in [25] that in the BDR interactions with the target select configurations in the projectile wave function where the projectile's energy is split between constituents much more efficiently than in the DGLAP regime. The simplest example is inclusive production of the leading hadrons in DIS for $Q \leq 2p_{\rm t}\,(\mathrm{BDR})$. Interactions with the target are not suppressed up to $p_{\rm t} \sim p_{\rm t}\,(\mathrm{BDR})$, leading to selection of configurations in γ^*, where longitudinal fractions carried by quark and antiquark are comparable. The photon energy splits between the partons **before** the collision. It is the interaction that selects at different energies different set of configurations which are resolved. Hence we refer to this phenomenon as the postselection. As a result, to a first approximation the leading hadrons are produced in the independent fragmentation of q and $\bar{q}$

$$\bar{D}^{\gamma_{\mathrm{T}}^{*}\to h}(z) = 2\int\limits_{z}^{1} dy D_q^h(z/y)\tfrac{3}{4}\left(1+(2y-1)^2\right) \tag{24}$$

leading to a strong suppression of the hadron production at $x_{\mathrm{F}} > 0.3$.

In the case of a parton of a hadron projectile propagating through the nucleus near BDR effective energy losses were estimated in Ref. [26]. For quarks they are expected to be of the order of 10% in the regime of the onset of BDR and larger deep inside this regime. Also the effective energy losses are somewhat larger for gluons as the $g \to gg$ splitting is more symmetric in the light cone fractions than the qg splitting.

8. Leading hadron production in hadron–nucleus scattering

Production of leading hadrons with $p_{\mathrm{t}} \sim$ few GeV/c in hadron–nucleus scattering at high energies provides a sensitive test of the onset of the BDR dynamics. Indeed in this limit pQCD provides a good description the forward single inclusive pion production in pp scattering at RHIC [27]. At the same time it was found to overestimate grossly the cross-section of the pion production in dAu collisions at RHIC in the same kinematics. The analysis of [28] has demonstrated that the dominant mechanism of the single pion production in the NN collisions in the kinematics studied at RHIC is scattering of leading quarks of the nucleon off the gluons of the target with the median value of x_g for the gluons to be in the range $x_g \sim 0.01 \div 0.03$ depending on the rapidity of the pion. The nuclear gluon density for such x is known to be close to the incoherent sum of the gluon fields of the individual nucleons since the coherent length in the interaction is rather modest for such x. As a result, the leading twist nuclear shadowing effects can explain only a very small fraction of the observed suppression [28] and one needs a novel dynamical mechanism to suppress generation of pions in such collisions. It was pointed out in [28] that the energy fractional energy losses on the scale of 10% give a correct magnitude of suppression of the inclusive spectrum due to a steep fall of the cross-section with x_{F} which is consistent with the estimates within the postselection mechanism.

An important additional information comes from the correlations studies where correlation of the leading pion with the pion produced at the central rapidities x [29, 30] which corresponds to the kinematics which receives the dominant contribution from the scattering off gluons with $x_g \sim 0.01 \div 0.02$. The rate of the correlations for pp scattering is consistent with pQCD expectations. An extensive analysis performed in [26] has demonstrated that the strengths of "hard forward pion"–"hard $\eta \sim 0$ pion" correlations in dAu and in pp scattering are similar. A rather small difference in the pedestal originates from the multiple soft collisions. Smallness of the increase of the soft pedestal as compared to pp collisions unambiguously demonstrates that the dominant source of the leading pions is the dAu scattering at large impact parameters. This conclusion is supported by the experimental observation [31] that the associated multiplicity of soft hadrons in events with forward pion is a factor of two smaller than in the minimum-bias dAu events. A factor of two reduction factor is consistent with the estimate of [26] based on the analysis of the soft component of $\eta = 0$ production for the forward pion trigger. Overall these data indicate that *(i)* the dominant source of the forward pion production is the $2 \to 2$ pQCD mechanism, *(ii)* production is dominated by projectile scattering at large impact parameters, *(iii)* proportion of small x_g contribution in the inclusive rate is approximately the same for pp and dAu collisions.

A lack of additional suppression of the $x_g \sim 0.01$ contribution to the double inclusive spectrum, as compared to the suppression of the inclusive spectrum, is explained in the post-selection mechanism as due to a relatively small momentum of the produced gluon in the nucleus rest frame, putting it far away from the BDR.

It is difficult to reconcile enumerated features of the forward pion production data with the $2 \to 1$ mechanism [32] inspired by the color glass condensate model. In the scenario of [32] incoherent $2 \to 2$ mechanism is neglected, a strong suppression of the recoil pion production is predicted. Also it leads to a dominance of the central impact parameters and hence a larger multiplicity for the central hadron production in the events with the forward pion trigger. The observed experimental pattern indicates the models [33] which neglect contribution of the $2 \to 2$ mechanism and consider only $2 \to 1$ processes strongly overestimates inclusive cross-section due to the $2 \to 1$ mechanism.

Overall the observed regularities of inclusive forward pion production and forward central correlation phenomenon give a strong indication of breakdown of the pQCD factorization due to the propagation of high energy partons through the nuclear media. The modification of the nuclear wave function at small $x < 0.01$ plays a small role in this kinematics.

9. Production of two forward pions and double-parton mechanism in *pp* and *dA* scattering

In Ref. [28] we suggested that in order to study the effects of small x gluon fields in the initial state one should study production of two leading pions in nucleon–nucleus collisions. Recently, the data were taken on production of two forward pions in dAu collisions. The preliminary results of the studies of the reactions $pp \to \pi^0\pi^0 + X$, d–Au $\to \pi^0\pi^0 + X$, where one leading pion served as a trigger and the second leading pion had somewhat smaller longitudinal and transverse momenta [34, 35]. The data indicate a strong suppression of the back-to-back production of pions in the central dAu collisions. Also a large fraction of the double inclusive cross-section is isotropic in the azimuthal angle $\Delta\varphi$ of the two pions.

We performed a study of this process in [36]. Our aims were to understand the origin of the suppression and, in particular, whether it is consistent with the postselection mechanism which explains the single inclusive and forward central data as well as the other features of the data.

9.1. Forward dipion production in pp scattering

It is instructive to start with the case of pp scattering. The leading twist contribution — $2 \to 2$ mechanism — corresponds to the process in which a leading quark from the nucleon and a small x gluon from the target scatter to produce two jets with leading pions. In this kinematics $x_g \leq M^2(\pi\pi)/x_q s_{NN}$. Production of two pions which together carry a large fraction of the nucleon momentum can occur only if x_q is sufficiently close to one. The results of our calculation show that the average value of x_q for typical cuts of the RHIC experiments is pretty close to one.

Obviously, it is more likely that two rather than one quark in a nucleon carry together x close to one. This suggests that in the discussed RHIC kinematics production the "double-scattering" contribution with two separate hard interactions in a single pp collision could become important. Hence though the discussed contribution is a "higher-twist", it is enhanced both by the probability of the relevant two quark configurations and the increase of the gluon density at small x which enters in the double-scattering in the second power.

One can derive the expression for the double-scattering mechanism based on the analysis of the corresponding Feynman diagrams and express it through the double generalized parton densities in the nucleons which we discussed in Sec. 4. Similar to Eq. (12) the cross-section can be written in the form

$$\frac{d^4\sigma}{dp_{\mathrm{T},1}d\eta_1 dp_{\mathrm{T},2}d\eta_2} = \frac{1}{\pi R^2_{\mathrm{int}}} \sum_{abcda'b'c'd'} \int dx_a dx_b dz_c dx_{a'} dx_{b'} dz_{c'}$$

$$\times f^{H_1}_{aa'}(x_a, x_{a'}) f^{H_2}_{b}(x_b) f^{H_2}_{b'}(x_{b'}) D^{h_1}_{c}(z_c)\, D^{h_1}_{c'}(z_{c'})\, \frac{d^2\hat{\sigma}^{ab\to cd}}{dp_{\mathrm{T},1}d\eta_1}\, \frac{d^2\hat{\sigma}^{a'b'\to c'd'}}{dp_{\mathrm{T},2}d\eta_2}\,. \quad (25)$$

Here $f^{H_1}_{aa'}(x_a, x_{a'})$ is the double parton distribution. If the partons are not correlated, it is equal to the product of the single parton distributions. For simplicity we neglected here correlations in the target as in our case xs for gluons are small. The dimensional factor πR^2_{int} is given by Eq. (15). In our numerical calculations we used $\pi R^2_{\rm int} \approx 15$ mb observed at the Tevatron which is smaller than the value obtained in the uncorrelated approximation (see discussion in Sec. 4).

We find that for the RHIC kinematics the only trivial correlation due to the fixed number of the valence quarks is important while the correlation between x_a and $x_{a'}$ remains a small correction if we follow the quark counting rules to estimate the $x_{a'}$ dependence off $f_{a,a'}(x_a, x_{a'})$ for fixed x_a. The results of our calculation indicate that the LT and double parton mechanisms are comparable for the kinematics of the RHIC experiments. This provides a natural explanation for the presence of a large component in the $pp \to \pi^0\pi^0 + X$ cross-section measured in [34, 35] which does not depend on the azimuth angle ϕ. In fact, the number of events in the pedestal comparable to the peak around $\phi \sim \pi$ which is dominated by the LT contribution indicating that the LT and double-parton contributions are indeed comparable (see Fig. 9 (a)).

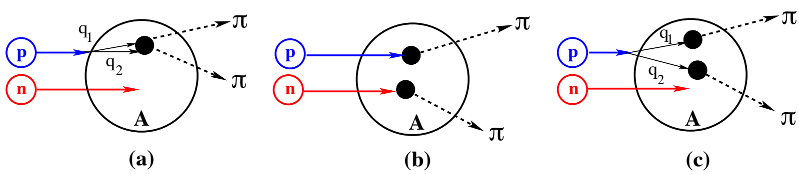

Fig. 9. Three double parton mechanisms of dipion production.

Hence we conclude that the current experiments at RHIC have found a signal of double-parton interactions and that future experiments at RHIC will be able to obtain a unique information about double quark distributions in nucleons. It will be crucial for such studies to perform analyses for smaller bins of η and preferably switch to the analysis in bins of Feynman x.

9.2. Production of two forward pions and double-parton mechanism in dAu scattering

Let us extend now our results to the case of d–A scattering studied at RHIC. In this case there are three distinctive double-parton mechanisms depicted in Fig. 9. The first two are the same as in the pA scattering–scattering of two partons of the nucleon off two partons belonging to different nucleons (mechanism (a)), and off two partons belonging to the same nucleon of the target (mechanism (b)) [38]. The third mechanism, which is not present for pA scattering is scattering of one parton of proton and one parton of the neutron off two partons of the nucleus. Let us consider the ratio of the double-parton and leading twist contributions for dA and pp collisions

$$r_{dA} = r_a + r_b + r_c = \frac{\sigma_{\rm DP}(dA)}{\sigma_{\rm LT}(dA)} \Big/ \frac{\sigma_{\rm DP}(pp)}{\sigma_{\rm LT}(pp)} \,. \tag{26}$$

The contribution to r_{dA} of the mechanisms (a), (c) is given by [38]

$$r_c = T(b)\sigma_{\rm eff}\,; \qquad r_a = 1\,, \tag{27}$$

where $T(b)$ is the standard nuclear profile function ($\int d^2bT(b) = A$). Here, we neglected nuclear gluon shadowing effect which is a small correction for the double-parton mechanism (*cf.* Ref. [28]) but maybe important for the LT mechanism, where x_g maybe as low as 10^{-3} due to the leading twist shadowing (see discussion below). For the central d–Au collisions $T_A \approx 2.2$ fm^{-2} and so $r_a/r_c \sim 1/3$. The contribution (b) can be calculated in a model independent way since no parton correlations enter in this case. The ratio of r_b and r_c will be close to 1 at midrapidity, where correlations and valence–gluon scattering are not very important. Toward large rapidities, however, r_b must become much larger than r_c, since it is not subject to the constraint $x_a + x_{a'} \leq 1$ because of the fact that for (b) the proton and the neutron scatter independently.

As a result, $r_{d\rm Au}$ for small b becomes of the order of ten r_A changes from ~ 9 to ~ 12 for $\pi R^2_{\rm int} = 15 \div 20$ mb.

Since the single inclusive pion spectrum for $\eta_2 \sim 2 \div 3$ is suppressed by a factor of the order of $R_A(b) = 1/3 \div 1/4$ we find for the ratio of the pedestals in dAu and pp

$$R_{\rm pedestal} = r_A R_A(b) \sim 2.5 \div 4 \tag{28}$$

which should be compared with the experimental value of $R_{\rm pedestal} \sim 3$. Hence we naturally explain the magnitude of the enhancement of the pedestal in central dAu collision (see horizontal (magenta) lines in Fig. 10).

If most of the pedestal in the kinematics studied at RHIC is due to the double-parton mechanism, the uncertainties in the estimate of the rates due to this mechanism and uncertainties in the strength of the suppression of the single inclusive forward pion spectrum at $b \sim 0$ would make it very difficult to subtract this contribution with a precision necessary to find out whether all pedestal is due to double-parton mechanism, or there is a room for a small contribution of the $2 \to 1$ broadening mechanism, as it was assumed in [37]. Note also that in [37] authors calculated the ratio of the double inclusive cross-section and the single inclusive cross-section in the color glass condensate approach and compared this ratio with the data. However, since the single inclusive spectrum is grossly overestimated by the model (see discussion in Sec. 8), such procedure is not legitimate.

The suppression of the away peak originating from the LT contribution is due to two effects: *(i)* the gluon shadowing for $x \sim 10^{-3}$ and $b \leq 3$ fm and $Q^2 \sim$ few GeV^2 reduces the cross-section by a factor of about two, *(ii)* stronger effect of effective fractional energy losses due to larger x of the quark in the LT mechanism than in the double parton mechanism, leading to a suppression factor of the order of two [36]. All together, this gives

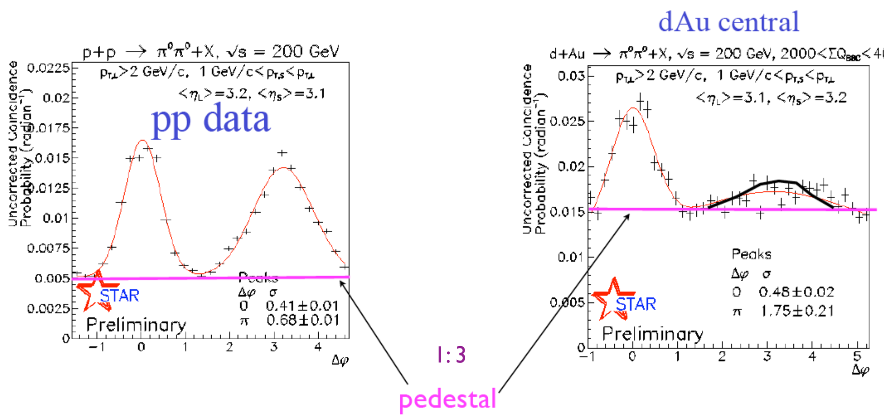

Fig. 10. STAR data for dipion production. Thin (red) curves are the Gaussian fit to the data. The horizontal (magenta) lines illustrate the strength of the double scattering, while the solid (black) curve in the dA plot illustrates the effect of the reduction of the $2 \to 2$ contribution by a factor of four, as compared to the pp case.

a suppression of the order of four as compared to the single pion trigger, which is consistent with the STAR observation — see solid curve in Fig. 10 (right). It corresponds to the overall suppression of the order of ten. This is pretty close to the low limit for the suppression estimated as the probability of the "punch through" mechanism — contribution from the process where a quark scatters off one nucleon but does not encounter any extra nucleons at its impact parameter. Probability of such collisions at $b \sim 0$ for interaction with Au nucleus is of the order of $5 \div 10\%$ [39].

The data are consistent with suppression of the away peak by a factor ≥ 4 and the reduction of the away peak relative to pedestal of the order of ten. The data may indicate that in addition to overall suppression there is some broadening of the away peak. Such effect is present in the postselection mechanism, though for the very forward kinematics it is a correction to the effective energy losses.

For the LHC kinematics the discussed effects will be grossly amplified and extend to much wider range of x — the same parton — target energy corresponds to rescaling of x of the factor of $s_{\mathrm{LHC}}/s_{\mathrm{RHIC}} \geq 10^3$. In addition, for $x \leq 0.1$ the gluons give the dominant contribution while the BDR scale of p_t^2 is about a factor of two larger in this case (*cf.* Fig. 8).

10. Conclusions

Studies aimed at understanding the underlying dynamics of pp scattering at the LHC energies face a number of challenges. The challenges discussed in this paper include:

1. Building models of inelastic collisions with realistic transverse parton distributions.
2. Including effects of the correlations between the partons in order to describe the rate of multiparton interactions.
3. Realistic modeling of the BDR effects at moderate transverse momenta.
4. Describing forward production at the LHC which is most sensitive to the BDR dynamics and, in particular, to the effect of effective fractional energy losses.

I thank my collaborators in the studies which form the basis of this paper: B. Blok, Yu. Dokshitzer, L. Frankfurt, V. Guzey, T. Rogers, W. Vogelsang, C. Weiss. My special thanks are to C. Weiss for critical reading of the first draft of the manuscript. The research was supported by the DOE grant No. DE-FG02-93ER40771.

REFERENCES

[1] J.C. Collins, L. Frankfurt, M. Strikman, *Phys. Rev.* **D56**, 2982 (1997).

[2] L. Frankfurt, M. Strikman, C. Weiss, *Phys. Rev.* **D69**, 114010 (2004).

[3] L. Frankfurt, M. Strikman, C. Weiss, *Phys. Rev.* **D83**, 054012 (2011) [`arXiv:1009.2559 [hep-ph]`].

[4] L. Frankfurt, C.E. Hyde, M. Strikman, C. Weiss, *Phys. Rev.* **D75**, 054009 (2007).

[5] M. Binkley *et al.*, *Phys. Rev. Lett.* **48**, 73 (1982).

[6] A. Siodmok, talk at the Workshop on the LHC Physics, Eugene, March 2011.

[7] For a summary, see: T. Sjostrand, P.Z. Skands, *Eur. Phys. J.* **C39**, 129 (2005).

[8] For a recent summary see: M. Bahr *et al.*, *Eur. Phys. J.* **C58**, 639 (2008).

[9] A.A. Affolder *et al.* [CDF Collaboration], *Phys. Rev.* **D65**, 092002 (2001).

[10] S. Chatrchyan *et al.* [CMS Collaboration], *J. High Energy Phys.* **1109**, 109 (2011) [`arXiv:1107.0330 [hep-ex]`].

[11] G. Aad *et al.* [ATLAS Collaboration], *Eur. Phys. J.* **C71**, 1636 (2011) [`arXiv:1103.1816 [hep-ex]`].

[12] Y.L. Dokshitzer, V.A. Khoze, A.H. Mueller, S.I. Troian, *Basics of Perturbative QCD*, Gif-sur-Yvette, France, Frontieres, 1991, p. 274.

[13] B. Blok, Y.L. Dokshitzer, L. Frankfurt, M. Strikman, *Phys. Rev.* **D83**, 071501 (2011) [`arXiv:1009.2714 [hep-ph]`].

[14] B. Blok, Y.L. Dokshitser, L. Frankfurt, M. Strikman, `arXiv:1106.5533 [hep-ph]`.

[15] V.M. Abazov *et al.* [D0 Collaboration], *Phys. Rev.* **D83**, 052008 (2011) [`arXiv:1101.1509 [hep-ex]`].

[16] L. Frankfurt, M. Strikman, D. Treleani, C. Weiss, *Phys. Rev. Lett.* **101**, 202003 (2008) [arXiv:0808.0182 [hep-ph]].

[17] M. Strikman, *Phys. Rev.* **D84**, 011501(R) (2011) [arXiv:1105.2285 [hep-ph]].

[18] F. Kramer, arXiv:1109.3383v1 [hep-ex]; P. Braun-Munzinger, lecture at the LI Cracow School of Theoretical Physics "Soft Side of the LHC".

[19] V. Khachatryan *et al.* [CMS Collaboration], *J. High Energy Phys.* **1009**, 091 (2010) [arXiv:1009.4122 [hep-ex]].

[20] L. Frankfurt, A. Radyushkin, M. Strikman, *Phys. Rev.* **D55**, 98 (1997) [arXiv:hep-ph/9610274].

[21] T. Rogers, V. Guzey, M. Strikman, X. Zu, *Phys. Rev.* **D69**, 074011 (2004).

[22] L. Frankfurt, V. Guzey, M. Strikman, arXiv:1106.2091 [hep-ph].

[23] T.C. Rogers, A.M. Stasto, M.I. Strikman, *Phys. Rev.* **D77**, 114009 (2008) [arXiv:0801.0303 [hep-ph]].

[24] T.C. Rogers, M. Strikman, *Phys. Rev.* **D81**, 016013 (2010) [arXiv:0908.0251 [hep-ph]].

[25] L. Frankfurt, V. Guzey, M. McDermott, M. Strikman, *Phys. Rev. Lett.* **87**, 192301 (2001) [arXiv:hep-ph/0104154].

[26] L. Frankfurt, M. Strikman, *Phys. Lett.* **B645**, 412 (2007) [arXiv:nucl-th/0603049].

[27] F. Aversa, P. Chiappetta, M. Greco, J.P. Guillet, *Nucl. Phys.* **B327**, 105 (1989); B. Jager, A. Schafer, M. Stratmann, W. Vogelsang, *Phys. Rev.* **D67**, 054005 (2003); D. de Florian, *Phys. Rev.* **D67**, 054004 (2003).

[28] V. Guzey, M. Strikman, W. Vogelsang, *Phys. Lett.* **B603**, 173 (2004).

[29] J. Adams *et al.* [STAR Collaboration], *Phys. Rev. Lett.* **97**, 152302 (2006).

[30] B. Meredith, *Nucl. Phys.* **A830**, 595 (2009) [arXiv:nucl-ex/0907.4832].

[31] G. Rakness, private communication.

[32] D. Kharzeev, E. Levin, L. McLerran, *Phys. Lett.* **B561**, 93 (2003) [arXiv:hep-ph/0210332]; D. Kharzeev, Y.V. Kovchegov, K. Tuchin, *Phys. Rev.* **D68**, 094013 (2003) [arXiv:hep-ph/0307037].

[33] A. Dumitru, A. Hayashigaki, J. Jalilian-Marian, *Nucl. Phys.* **A765**, 464 (2006).

[34] E. Braidot [STAR Collaboration], arXiv:1005.2378v1 [hep-ph].

[35] B. Meredith, *PoS* **(DIS 2010)**, 081 (2010).

[36] M. Strikman, W. Vogelsang, *Phys. Rev.* **D83**, 034029 (2011) [arXiv:1009.6123 [hep-ph]].

[37] J.L. Albacete, C. Marquet, *Phys. Rev. Lett.* **105**, 162301 (2010) [arXiv:1005.4065 [hep-ph]].

[38] M. Strikman, D. Treleani, *Phys. Rev. Lett.* **88**, 031801 (2002) [arXiv:hep-ph/0111468].

[39] M. Alvioli, H.J. Drescher, M. Strikman, *Phys. Lett.* **B680**, 225 (2009) and to be published.